Journal of Thrombosis and Thrombolysis (2018) 46:203–210
https://doi.org/10.1007/s11239-018-1697-z

The utility of total lipid core burden index/maximal lipid core burden index ratio within the culprit plaque to predict filter-no reflow: insight from near-infrared spectroscopy with intravascular ultrasound

Takao Sato[1] · Yoshifusa Aizawa[1] · Naomasa Suzuki[1] · Yuji Taya[1] · Sho Yuasa[1] · Shohei Kishi[1] · Tomoyasu Koshikawa[1] · Koichi Fuse[1] · Satoshi Fujita[1] · Yoshio Ikeda[1] · Hitoshi Kitazawa[1] · Minoru Takahashi[1] · Masaaki Okabe[1]

Published online: 18 June 2018

Abstract
Filter-no reflow (FNR) is a phenomenon wherein flow improves after the retrieve of distal protection. Near-infrared spectroscopy with intravascular ultrasound (NIRS–IVUS) enables lipid detection. We evaluated the predictors of FNR during PCI using NIRS–IVUS. Thirty-two patients who underwent PCI using the Filtrap® for acute coronary syndrome (ACS) were enrolled. The culprit plaque (CP) was observed using NIRS–IVUS. Total lipid-core burden index (T-LCBI) and maximal LCBI over any 4-mm segment (max-LCBI4mm) within CP were evaluated. T-LCBI/max–LCBI4mm ratio within CP was calculated as an index of the extent of longitudinal lipid expansion. The attenuation grade (AG) and remodeling index (RI) in CP were analyzed. AG was scored based on the extent of attenuation occupying the number of quadrants. The patients were divided into FNR group (N = 8) and no-FNR group (N = 24). AG was significantly higher in FNR group than in no-FNR group (1.6 ± 0.6 vs. 0.9 ± 0.42, p = 0.01). RI in FNR group tended to be greater than in no-FNR group. T-LCBI/max–LCBI4mm ratio within the culprit plaque was significantly higher in FNR group than in no-FNR group (0.50 ± 0.10 vs. 0.33 ± 0.13, p < 0.01). In multivariate logistic regression analysis, AG > 1.04 (odds ratio [OR] 18.4, 95% confidence interval [CI] 1.5–215.7, p = 0.02) and T-LCBI/max–LCBI4mm ratio > 0.42 (OR 14.4, 95% CI 1.2–176.8, p = 0.03) were independent predictors for the occurrence of FNR. The use of T-LCBI/max–LCBI4mm ratio within CP might be an effective marker to predict FNR during PCI in patients with ACS.

Keywords Filter no-reflow · NIRS–IVUS · Percutaneous coronary intervention

Highlights

- LCBI value within the culprit plaque in the FNR group was significantly higher than in the no-FNR group
- Multiple logistic regression revealed that T-LCBI/max-LCBI4mm ratio within the culprit plaque and attenuation grade were independent predictors for FNR
- In future, the proper length of max–LCBI to evaluate vulnerable plaque should evaluated using next-generation NIRS-IVUS

✉ Takao Sato
kirotaro19731013@yahoo.co.jp

[1] Cardiology, Tachikawa General Hospital, 561-1 Jyojyomachi Aza Yauchi, Nagaoka, Japan

Introduction

Percutaneous coronary intervention (PCI) may be complicated by peri-procedural myocardial infarction and reduced antegrade flow ("no-reflow"), which has been shown to be associated with worse short- and long-term clinical outcomes [1]. No-reflow is attributable to the distal embolization of atheromatous or thrombotic materials that derives from mechanical fragmentation of the culprit plaque by PCI. Several studies have demonstrated that thrombus formation, positive remodeling, and greater lipid plaque burden were independent predictors of the no-reflow phenomenon [2].

Furthermore, filter-no reflow (FNR) is a phenomenon wherein flow improves after the retrieve of distal protection. However, the usefulness of distal protection remains controversial [3, 4]. Conversely, some studies showed that distal protection devices may improve myocardial reperfusion among selected high-risk patient groups [5, 6].

While, combined imaging with near-infrared spectroscopy (NIRS) and intravascular ultrasound (IVUS) enables the identification and morphometric assessment of lipid-rich plaques in vivo [7]. This dual modality catheter was validated by prior studies in the setting of acute coronary syndrome (ACS) [8, 9]. A previous autopsy study demonstrated that NIRS was able to detect features associated with plaque vulnerability in humans [10]. In fact, a maximal lipid core burden index4mm (max-LCBI4mm) > 400 in NIRS accurately distinguished culprit from non-culprit segments within the artery [9].

Thus, the present study aimed to evaluate the prediction of the FNR phenomenon during PCI by using near-infrared spectroscopy with intravascular ultrasound (NIRS–IVUS).

Methods

Study population

Thirty-two patients who underwent PCI under distal protection device for ACS were prospectively enrolled. Patients had ischemic chest discomfort with ST-segment elevation or depression of > 0.5 mm or T-wave inversion in 2 or more leads. Acute myocardial infarction was diagnosed by increased troponin T, serum levels of creatine phosphokinase (CPK) (more than twice the upper limit of normal), and creatine phosphokinase-MB fraction (> 10% of total creatine kinase). Patients without elevation of the creatine kinase-MB fraction were classified as having unstable angina.

Patients with the following criteria were excluded: cardiogenic shock, left main coronary artery disease, extremely tortuous or heavily calcified vessels, intolerance to antiplatelet drugs, in-stent restenosis after DES implantation, and severe chronic kidney disease (an estimated glomerular filtration rate < 30 ml/min/1.73 m^2).

Our study was approved by our institutional ethics review board and all participants provided written informed consent for the use of their data in our retrospective analysis.

PCI procedure

Patients who had undergone emergent PCI in this study presented to the emergency room with suspected ACS. Aspirin (200 mg) was administered orally in the emergency room, followed by a daily maintenance per oral dose of 100 mg thereafter. In addition, patients were also administered clopidogrel or prasugrel, at a loading dose of 300 or 20 mg, respectively, with a daily maintenance per oral dose of 75 mg for clopidogrel and 3.75 mg for prasugrel thereafter. Thereafter, dual anti-platelet therapy (DAPT) was continued for at least 1 year after PCI. Furthermore, unfractionated heparin was administered intravenously to achieve an activated clotting time of 200–250 s during PCI. A 6-French arterial sheath and a transradial or transfemoral artery approach were utilized. Angiography was performed using a 6-F guiding catheter to identify the site of the culprit lesion. A 0.014-inch coronary guidewire was passed through the lesion. After thrombus aspiration, a filter-based distal protection device (Filtrap®; NIPRO, Osaka, Japan), was placed distal to the culprit lesion. Based on operator's discretion, a pre-dilatation procedure was also performed. Thereafter, after intravascular evaluation by NIRS–IVUS, a stent was implanted at the culprit plaque. Post-dilatation procedures were also performed based on NIRS–IVUS assessment with the objective of achieving optimal results. After completion of the PCI procedure, the Filtrap® was removed from the patient. Thereafter, the weight of the debris retrieved by the distal protection devices was evaluated. After stent implantation, thrombolysis myocardial infarction trial (TIMI) grade was evaluated and peak CPK was also followed.

Image acquisition by NIRS (Fig. 1)

In the present study, the TVC catheter (InfraReDx, Inc., Burlington, Massachusetts), a dual-modality intravascular imaging device that coregisters a NIRS chemogram to a gray-scale IVUS image, was used to analyze culprit lesion. NIRS–IVUS was performed with a 3.2-F TVC catheter from the distal target vessel to the guide catheter using a motorized pullback system at 0.5 mm/s. In the present study, the culprit plaque was defined as the site of stent implantation; the site was identified using any markers such as side branches and calcification and observed before and after stent implantation. The total lipid core burden index (T-LCBI) and max-LCBI4mm within the culprit plaque were then automatically calculated as previously described [11]. In addition, to express the longitudinal expansion of the lipid within the culprit plaque, the T-LCBI/max–LCBI4mm ratio within the culprit plaque was also calculated. If the lipid arc in the entire culprit plaque is the same as that in the max-LCBI4mm, the T-LCBI/max–LCBI4mm ratio results in a value of 1. NIRS signal was measured before balloon dilatation of any type. However, based on the discretion of the clinical operator, the NIRS measurement was performed after pre-dilatation. NIRS data were stored digitally for subsequent analysis.

Gray-scale intravascular ultrasound image analysis (Fig. 1)

Quantitative analysis was performed according to the American College of Cardiology clinical expert consensus document on IVUS [12] cross-sectional area (CSA) of the lumen and the vessel was determined at the reference as well as the culprit lesion site manually. Vessel

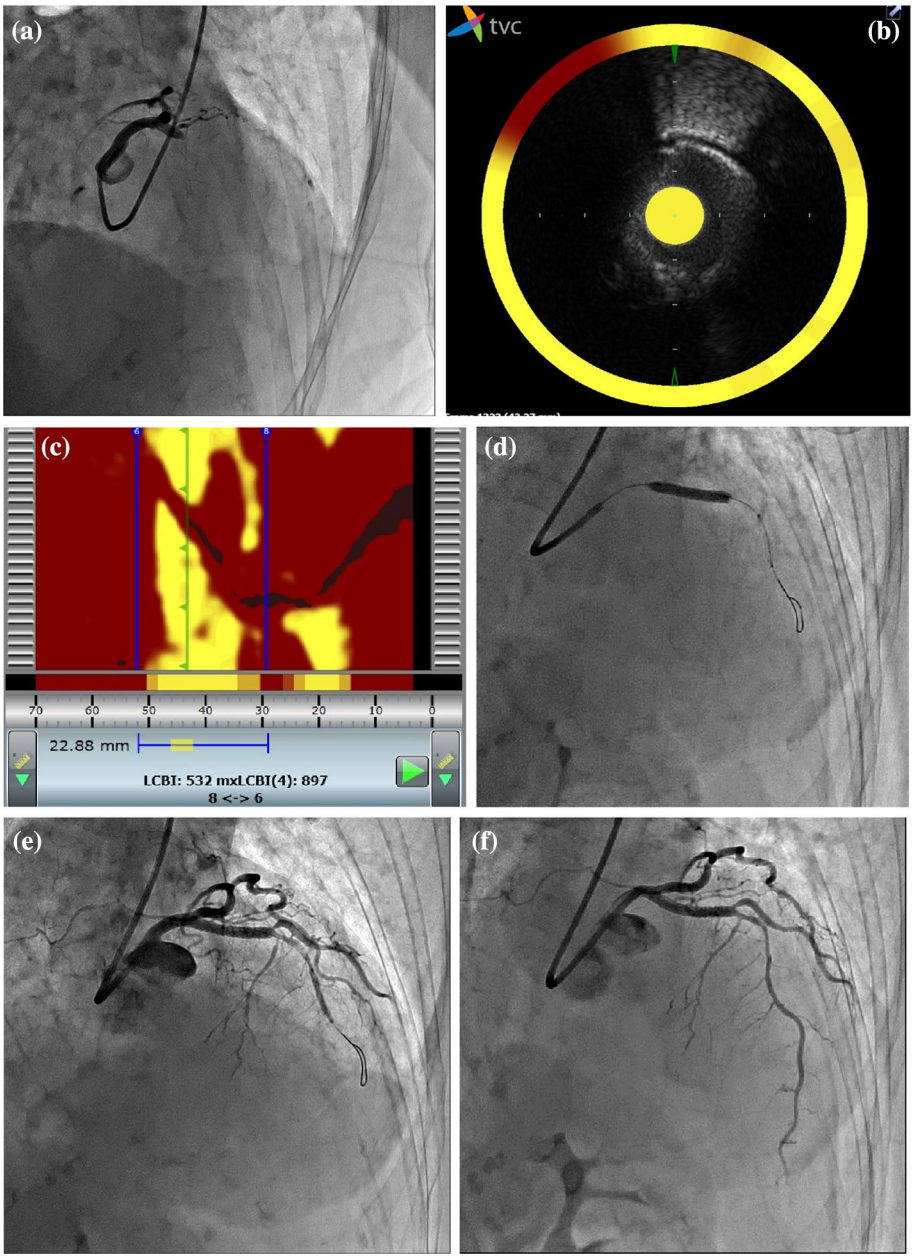

Fig. 1 A representative data. A 98-year-old female patient with ST elevated myocardial infarction who had 100% occlusion in the left anterior descending artery is shown (**a**). NIRS–IVUS (**b, c**) shows the attenuation of grade 4, and T-LCBI, max-LCBI4mm and T-LCBI/max–LCBI4mm ratio in culprit plaque (T-LCBI, max-LCBI4mm and T-LCBI/max–LCBI4mm ratio were 532, 897 and 0.59, respectively). Stent implantation (**d**) was performed. Coronary angiogram after stent implantation (**e**) shows filter-no flow. Coronary angiogram after the retrieve of distal protection (**f**) shows improvement in antegrade flow

CSA was determined with the external elastic membrane (EEM) as the outer margin of the vessel, and lumen CSA, with the lumen border as the outer margin of the lumen. The difference between vessel CSA and lumen CSA thus provided the CSA of the plaque + media. The percentage of CSA of plaque + media was calculated as an index of plaque burden by dividing the CSA of the plaque + media by the vessel CSA. The proximal and distal reference segments were defined as the segments with the largest lumen with the least plaque and located within 5 mm proximal and distal to the lesion, but proximal to a major side branch [13]. The remodeling index (RI) was calculated by dividing the EEM CSA at the culprit lesion by the mean of the proximal and distal reference CSA. Remodeling with an RI > 1.05 was defined as positive remodeling, whereas remodeling with an RI < 0.95 was defined as negative remodeling [14].

Attenuation was defined as the backward signal attenuation without dense calcium [15] and the grade was scored based on the extent of attenuation occupying the number of quadrants as follows: grade 0, no attenuation; grade 1, 1-quadrant (< 90°); grade 2, 2-quadrant (90°–179°), grade 3, 3-quadrant (180°–269°); grade 4, 4-quadrant (270°–360°) attenuation.

Statistical analyses

All statistical analyses were performed using SPSS version 22 (IBM Japan, Tokyo, Japan). Continuous data with non- normal distribution are presented as means ± standard deviation, and categorical data as count percentages. The patients were divided into the FNR (N = 8) and no-FNR groups (N = 24). Comparisons between the FNR group and the no-FNR group were performed by Mann–Whitney's U test for continuous data and Fisher's exact test for categorical data. In addition, the area under curve (AUC) by receiver-operating characteristic (ROC) curve analysis using T-LCBI, max-LCB4mm, and the T-LCBI/max–LCBI4mm ratio was calculated. This was done to clarify a marker with high accuracy for predicting the occurrence of FNR. As a result, the AUC of T-LCBI/max–LCBI4mm ratio was greatest among T-LCBI, max-LCB4mm, and the T-LCBI/max–LCBI4mm ratio (AUC = 0.868, AUC = 0.864, and AUC = 0.885, respectively). Therefore, using the T-LCBI/max–LCBI4mm ratio, multiple logistic regression analysis was performed to determine the independent predictor for the occurrence of FNR. In addition, ROC curve analysis was conducted to identify the best cut-off value of T-LCBI/max–LCBI4mm ratio for predicting the occurrence of FNR. The best cut-off value was determined using the maximum sum of sensitivity and specificity. A two-sided p-value of < 0.05 was considered statistically significant for all analyses.

Results

Patient characteristics (Table 1)

The patients' mean age was 67 ± 10 years. Men comprised 67% of patients. Overall, the frequency of FNR was 25%. There were no significant differences in age, body mass index, and medical history, including hypertension, dyslipidemia, diabetes mellitus, and smoking between 2 groups.

Table 1 Baseline characteristics

	All (N = 32)	FNR (N = 8)	No FNR (N = 24)	P value
Age (years)	70.3 ± 13.5	74.6 ± 17.0	67.2 ± 10.7	0.42
Male	28 (87.5)	7 (87.5)	20 (83.3)	0.78
BMI	23.5 ± 3.3	23.0 ± 3.0	23.8 ± 3.7	0.69
Hypertension	24 (75)	5 (62.5)	19 (79.1)	0.42
Dyslipidemia	23 (72)	5 (62.5)	18 (75.0)	0.55
Diabetes mellitus	10 (31.2)	2(25.0)	8 (33.3)	0.67
Smoking ever	12 (37.5)	2 (25.0)	10 (41.6)	0.40

Data are presented as mean ± SD or n (%)

BMI body mass index

Difference between both groups (Table 2)

Regarding PCI procedure, the use of thrombus aspiration, and frequency of pre-dilatation and post-dilatation were comparable between groups. Regarding IVUS data, the attenuation grade was significantly higher in the FNR group than in the no-FNR group (1.6 ± 0.6 vs. 0.9 ± 0.42, p < 0.01). Plaque burden was comparable between groups (66.3 ± 7.4 vs. 66.4 ± 3.8%, p = 0.98). However, RI in the FNR group tended to be higher than in the no-FNR group (1.18 ± 0.22 vs. 1.06 ± 0.04, p = 0.08). Lumen area and vessel area were also similar between both groups.

As for, NIRS, max-LCBI4mm, T-LCBI, and the T-LCBI/max–LCBI4mm ratio were significantly higher in the FNR group than in the no-FNR group (559 ± 160 vs. 351 ± 140, p = 0.01; 285 ± 125 vs. 116 ± 105, p = 0.01; 0.50 ± 0.10 vs. 0.33 ± 0.13, p < 0.01). In addition, the weight of the retrieved debris was significantly heavier in the FNR group than in the no-FNR group (11.1 ± 3.2 vs. 7.0 ± 2.4 mg, p < 0.01).

TIMI grade at final angiography was also similar between groups. In addition, there was no significant difference in peak CPK value between groups (2825 ± 2016 vs. 2329 ± 1109 IU/L, p = 0.73).

The predictor for the occurrence of FNR (Table 3)

To identify predictors for the occurrence of FNR and parameters with a p-value for univariate analysis < 0.10, i.e., attenuation grade, RI and T-LCBI/max–LCBI4mm ratio were selected for the multivariate logistic regression analyses. The variables were stratified according to their average value (attenuation grade > 1.04, RI > 1.07, T-LCBI/max–LCBI4mm ratio > 0.42). Multivariate logistic regression analysis revealed that attenuation grade > 1.04 (odds ratio [OR] 18.4, 95% confidence interval [CI] 1.5–215.7, p = 0.02) and T-LCBI/max–LCBI4mm ratio > 0.42 (OR 14.4, 95% CI 1.2–176.8, p = 0.03) were significant positive predictors for the occurrence of FNR (Table 4).

The cut-off value of T-LCBI/max–LCBI4mm ratio for predicting the occurrence of FNR (Fig. 2)

Receiver operating characteristic curve analysis revealed a cut-off value of 0.47 for T-LCBI/max–LCBI4mm ratio predicting the occurrence of FNR (AUC = 0.88; sensitivity, 87.5%; specificity, 74.0%).

Table 2 The data during PCI

	FNR (N = 8)	Non-FNR (N = 24)	P value
LAD/LCX/RCA (n)	7/0/1	11/3/10	0.11
Aspiration	5 (61.5)	16 (66.6)	0.84
Pre dilatation	5 (61.5)	13 (54.1)	0.70
Stent implantation			
Size (mm)	3.4 ± 0.42	3.2 ± 0.6	0.55
Length (mm)	22.2 ± 8.5	26.8 ± 5.8	0.32
Post dilatation	7 (87.5)	18 (75.0)	0.43
IVUS			
Lumen (mm^2)	4.8 ± 1.5	4.8 ± 1.7	0.94
Vessel (mm^2)	15.4 ± 5.4	14.5 ± 4.8	0.63
% plaque	66.3 ± 7.4	66.4 ± 3.4	0.98
Attenuation grade	1.6 ± 0.5	0.9 ± 0.5	< 0.01
Remodeling index	1.18 ± 0.22	1.06 ± 0.04	0.08
NIRS before PCI			
Max-LCBI4mm	559 ± 160	351 ± 140	0.01
T-LCBI	285 ± 125	116 ± 106	0.01
T-LCBI/max–LCBI4mm ratio	0.50 ± 0.10	0.33 ± 0.13	< 0.01

Data are presented as mean ± SD or n (%)

FNR filter no reflow, *LAD* left anterior descending artery, *LCX* circumflex artery, *RCA* right coronary artery, *IVUS* intravascular ultrasound, *PCI* percutaneous coronary intervention, *LCBI* lipid core burden index

Table 3 The data after PCI

	FNR (N = 8)	No FNR (N = 24)	P value
NIRS after PCI			
Max-LCBI4mm	174 ± 142	166 ± 114	0.91
T-LCBI	91 ± 64	43 ± 37	0.20
T-LCBI/max–LCBI4mm ratio	0.53 ± 0.16	0.23 ± 0.06	0.01
Final TIMI grade (n)			0.25
0	0	0	
1	0	0	
2	1	0	
3	7	24	
Peak CPK (IU/L)	2825 ± 2016	2329 ± 1109	0.73
Debris weight (mg)	11.1 ± 3.2	7.0 ± 2.4	< 0.01

Data are presented as mean ± SD

FNR filter no reflow, *PCI* percutaneous coronary intervention, *LCBI* lipid core burden index, *TIMI* thrombolysis in myocardial infarction trial, *CPK* creatine phosphokinase

Table 4 Multiple logistic regression analysis for the independent predictor of the occurrence of FNR

	Odds ratio	95% CI	P value
Remodeling index > 1.07	1.87	0.17–20.5	0.60
Attenuation grade > 1.04	18.4	1.5–215.7	0.02
T-LCBI/max–LCBI4mm > 0.4	14.4	1.2–176.8	0.03

CI confidence interval, *LCBI* lipid core burden index

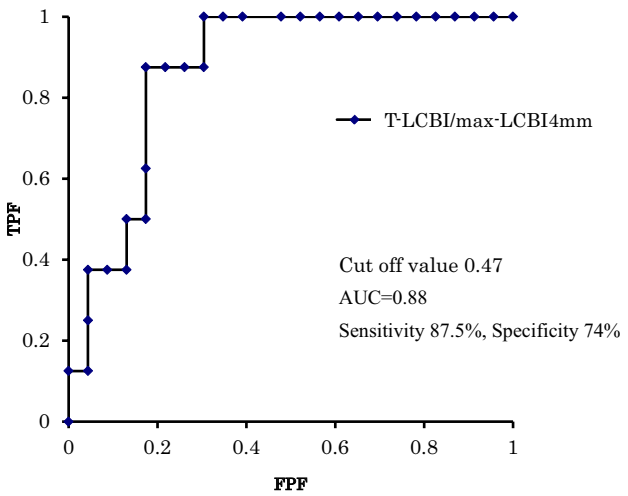

Fig. 2 Receiver operating characteristic curve analysis for predicting FNR. The cut-off value of T-LCBI/max–LCBI4mm ratio for predicting the occurrence of FNR is shown. See text for details

Discussion

The main findings of the present study are as follows: (1) LCBI value within the culprit plaque in the FNR group was significantly higher than in the no-FNR group, and (2) multiple logistic regression revealed that T-LCBI/

max–LCBI4mm ratio within the culprit plaque and attenuation grade were independent predictors for FNR.

Validation between NIRS and lipid plaque

Vulnerable plaques are typically characterized by large necrotic cores with either a nonexistent or a thin cap fibrous (< 65 μm) and active macrophages near or within the fibrous cap [16, 17]. The necrotic core of the atherosclerotic plaque is highly thrombogenic and contains fragile tissues such as lipid depositions within foam cells as well as intramural bleeding and/or cholesterol crystals [18].

To validate the accuracy of the NIRS catheter for detection of lipid core plaque, two pivotal studies including the SPECTACL clinical study were carried out. These studies validated the NIRS catheter for accuracy in detection of lipid core plaque [19, 20]. In fact, a study using coronary angiography and NIRS showed that the culprit lesions of ACS were lipid core plaques (84.4%) in most cases [21]. Furthermore, in a study of 20 patients with ST-segment elevation myocardial infarction, max-LCBI4mm > 400 in NIRS accurately distinguished culprit segment from non-culprit segments within the artery [19]. A larger patient group during a multicenter trial reported similar results [22]. Moreover, our study also showed that mean max-LCBI4mm of culprit plaque in the patients with ACS was nearly 400, which is compatible with above-mentioned data. Thus, it is expected that this novel capability of NIRS will be of assistance in the management of patients with coronary artery disease.

The relationship among NIRS, lipid and FNR

As mentioned, the necrotic core plaque is highly thrombogenic, containing fragile tissues such as lipid depositions within foam cells [18]. These elements may be related to instent thrombus formation [23] or can be easily released into the blood stream during coronary interventions [24–26]. One cause of peri-procedural myocardial infarction is attributable to distal embolization of these lipid core plaque contents and/or intracoronary thrombus [27].

In addition, the no-reflow phenomenon is originally described as an angiographic phenomenon that occurs when inadequate myocardial perfusion is observed after opening an epicardial coronary artery with stenosis; regardless of the underlying causes, no-reflow phenomenon is related to long-term mortality in patients with STEMI [28, 29]. In general, this phenomenon is now understood to be caused by multiple factors including endothelial dysfunction, myocyte edema, neutrophil infiltration, microvascular spasm, oxygen-free radicals, and distal embolization of plaque and/or thrombus at culprit coronary lesion [30]. The distal atherothrombotic embolization has been reported to contribute to microvascular injury to some extent, particularly during PCI [15]. So far, there are various reports on the predictor of FNR, slow flow, and no-reflow using various imaging device such as IVUS, magnetic resonance imaging, and OCT [2, 15, 31–35]. Several reports have shown that atherosclerotic plaque with ultrasound attenuation might be related to the deterioration of coronary flow in patients with ACS. In fact, in several autopsy studies, ultrasound attenuation was associated with fibro-fatty tissue containing scattered cholesterol clefts and Von Kossa-positive granules corresponding to microcalcification [36, 37]. Therefore, in the present study, the high attenuation grade and high LCBI value relationship to FNR agrees with these reports. Among these risk factors for the deterioration of coronary flow, distal embolization of the contents of the plaque and/or thrombus might be prevented. Therefore, the effect of distal protection devices has been studied. However, the effect of distal protection devices was controversial [3, 4, 38, 39]. Therefore, it is important to predict the necessity of distal protection device during PCI because various imaging modalities have demonstrated an association between PCI of lipid core plaque and periprocedural MI [18, 40–44]. As with these imaging devices, several NIRS–IVUS studies has also described that high LCBI value, including T-LCBI and max-LCBI4mm, was associated with a high risk of periprocedural MI, presumably due to distal embolization [11, 24, 45]. In addition, the dilation of a large, longitudinal and circumferential lipid core lesion was associated with a high risk of periprocedural MI [24]. Because the T-LCBI/max–LCBI4mm ratio within the culprit plaque adopted in our study indicates the longitudinal and circumferential lipid expansion, the high T-LCBI/max–LCBI4mm ratio causing the occurrence of the FNR seems to agree with these reports. Additionally, the change in LCBI value before and after stent implantation was significantly greater in the FNR group than in no-FNR group. In addition, the present study has shown that T-LCBI/max–LCBI4mm ratio within the culprit plaque was also associated with heavy weight of debris retrieved from distal protection. Therefore, a randomized study would be required to determine whether NIRS can prospectively identify lipid core plaque prone to a high rate of distal embolization and periprocedural MI, and whether the use of a distal protection device is effective in preventing this complication.

Limitations

Limitations of this study are as follows. First, the number of study patients was small, although this is a prospective study. Second, as it had been already reported that the attenuation plaque on IVUS, T-LCBI, and max-LCBI4mm values were associated with a high incidence of transient no-reflow; we conducted a study using distal protection device to investigate the predictors such as T-LCBI/max–LCBI4mm ratio associated with FNR phenomenon, regardless of the lack of

periprocedural myocardial enzyme examinations. In addition, NIRS cannot evaluate the depth of the lipid pool [46]. Therefore, another modality like optical coherence tomography should be utilized in future study. Third, distal protection device and NIRS–IVUS catheter were not used in all lesions for the following reasons: severe tortuousness, small vessel diameter, severity of stenosis, and the presence of severe calcification. Consequently, our results were limited by selection bias and may not apply to such lesions. Therefore, no definite conclusion can be drawn from the results of the present study. These limitations warrant future studies involving larger populations.

Conclusion

The use of T-LCBI/max–LCBI4mm ratio within the culprit plaque by NIRS–IVUS might be an effective marker to predict FNR during PCI.

Compliance with ethical standards

Conflict of interest The authors declare that there is no conflict of interest.

Ethical approval Our study was approved by our institutional ethics review board and all participants provided written informed consent for the use of their data in our retrospective analysis.

References

1. Watabe H, Sato A, Akiyama D, Kakefuda Y, Adachi T, Ojima E et al (2012) Impact of coronary plaque composition on cardiac troponin elevation after percutaneous coronary intervention in stable angina pectoris: a computed tomography analysis. J Am Coll Cardiol 59:1881–1888
2. Matsumoto K, Ehara S, Hasegawa T, Otsuka K, Yoshikawa J, Shimada K (2016) Prediction of the filter no-reflow phenomenon in patients with angina pectoris by using multimodality: magnetic resonance imaging, optical coherence tomography, and serum biomarkers. J Cardiol 67:430–436
3. Stone GW, Webb J, Cox DA, Brodie BR, Qureshi M, Kalynych A et al (2005) Distal microcirculatory protection during percutaneous coronary intervention in acute ST-segment elevation myocardial infarction: a randomized controlled trial. JAMA 293:1063–1072
4. Kaltoft A, Kelbaek H, Kløvgaard L, Terkelsen CJ, Clemmensen P, Helqvist S et al (2010) Increased rate of stent thrombosis and target lesion revascularization after filter protection in primary percutaneous coronary intervention for ST-segment elevation myocardial infarction: 15-month followup of the DEDICATION (Drug Elution and Distal Protection in ST Elevation Myocardial Infarction) trial. J Am Coll Cardiol 55:867–871
5. Limbruno U, Micheli A, De Carlo M, Amoroso G, Rossini R, Palagi C et al (2003) Mechanical prevention of distal embolization during primary angioplasty: safety, feasibility, and impact on myocardial reperfusion. Circulation 108:171–176
6. Mizote I, Ueda Y, Ohtani T, Shimizu M, Takeda Y, Oka T et al (2005) Distal protection improved reperfusion and reduced left ventricular dysfunction in patients with acute myocardial infarction who had angioscopically defined ruptured plaque. Circulation 112:1001–1007
7. Puri R, Madder RD, Madden SP, Sum ST, Wolski K, Muller JE et al (2015) Near-infrared spectroscopy enhances intravascular ultrasound assessment of vulnerable coronary plaque: a combined pathological and in vivo study. Arterioscler Thromb Vasc Biol 35:2423–2431
8. Madder RD, Puri R, Muller JE, Harnek J, Götberg M, VanOosterhout S et al (2016) Confirmation of the intracoronary near-infrared spectroscopy threshold of lipid-rich plaques That underlie ST-segment-elevation myocardial infarction. Arterioscler Thromb Vasc Biol 36:1010–1015
9. Madder RD, Goldstein JA, Madden SP, Puri R, Wolski K, Hendricks M et al (2013) Detection by near-infrared spectroscopy of large lipid core plaques at culprit sites in patients with acute ST segment elevation myocardial infarction. JACC Cardiovasc Interv 6:838–846
10. Roleder T, Kovacic JC, Ali Z, Sharma R, Cristea E, Moreno P et al (2014) Combined NIRS and IVUS imaging detects vulnerable plaque using a single catheter system: a head-to-head comparison with OCT. EuroIntervention 10:303–311
11. Goldstein JA, Maini B, Dixon SR, Brilakis ES, Grines CL, Rizik DG et al (2011) Detection of lipid-core plaques by intracoronary near-infrared spectroscopy identifies high risk of periprocedural myocardial infarction. Circ Cardiovasc Interv 4:429–437
12. Mintz GS, Nissen SE, Anderson WD, Bailey SR, Erbel R, Fitzgerald PJ et al (2001) American College of Cardiology Clinical Expert Consensus Document on Standards for Acquisition, Measurement and Reporting of Intravascular Ultrasound Studies (IVUS). A report of the American College of Cardiology Task Force on Clinical Expert Consensus Documents. J Am Coll Cardiol 37:1478–1492
13. Wu X, Maehara A, Mintz GS, Kubo T, Xu K, Choi SY et al (2010) Virtual histology intravascular ultrasound analysis of non-culprit attenuated plaques detected by grayscale intravascular ultrasound in patients with acute coronary syndromes. Am J Cardiol 105:48–53
14. Pasterkamp G, Borst C, Gussenhoven EJ, Mali WP, Post MJ, The SH et al (1995) Remodeling of de novo atherosclerotic lesions in femoral arteries: impact on mechanism of balloon angioplasty. J Am Coll Cardiol 26:422–428
15. Endo M, Hibi K, Shimizu T, Komura N, Kusama I, Otsuka F et al (2010) Impact of ultrasound attenuation and plaque rupture as detected by intravascular ultrasound on the incidence of no-reflow phenomenon after percutaneous coronary intervention in ST-segment elevation myocardial infarction. JACC Cardiovasc Interv 3:540–549
16. Narula J, Nakano M, Virmani R, Kolodgie FD, Petersen R, Newcomb R et al (2013) Histopathologic characteristics of atherosclerotic coronary disease and implications of the findings for the invasive and noninvasive detection of vulnerable plaques. J Am Coll Cardiol 61:1041–1051
17. Van der Wal AC, Becker AE (1999) Atherosclerotic plaque rupture–pathologic basis of plaque stability and instability. Cardiovasc Res 41:334–344
18. Kawamoto T, Okura H, Koyama Y, Toda I, Taguchi H, Tamita K et al (2007) The relationship between coronary plaque characteristics and small embolic particles during coronary stent implantation. J Am Coll Cardiol 50:1635–1640
19. Gardner CM, Tan H, Hull EL, Lisauskas JB, Sum ST, Meese TM et al (2008) Detection of lipid core coronary plaques in autopsy specimens with a novel catheter-based nearinfrared spectroscopy system. JACC Cardiovasc Imaging 1:638–648

20. Waxman S, Dixon SR, L'Allier P, Moses JW, Petersen JL, Cutlip D et al (2009) In vivo validation of a catheter-based near-infrared spectroscopy system for detection of lipid core coronary plaques: initial results of the SPECTACL study. JACC Cardiovasc Imaging 2:858–868
21. Madder RD, Smith JL, Dixon SR, Goldstein JA (2012) Composition of target lesions by near-infrared spectroscopy in patients with acute coronary syndrome versus stable angina. Circ Cardiovasc Interv 5:55–61
22. Madder RD, Muller JE, Puri R, Harnek J, Gotberg M, McNamara RF et al (2013) TCT-660 multicenter validation of a near-infrared spectroscopic signature of culprit lesions causing ST-segment elevation myocardial infarction: the NIRSTEMI II study. J Am Coll Cardiol 62:B201
23. Papayannis AC, Abdel-Karim AR, Mahmood A, Rangan BV, Makke LB, Banerjee S et al (2013) Association of coronary lipid core plaque with intrastent thrombus formation: a near-infrared spectroscopy and optical coherence tomography study. Catheter Cardiovasc Interv 81:488–493
24. Goldstein JA, Grines C, Fischell T, Virmani R, Rizik D, Muller J et al (2009) Coronary embolization following balloon dilation of lipid-core plaques. JACC Cardiovasc Imaging 2:1420–1424
25. Schultz CJ, Serruys PW, van der Ent M, Ligthart J, Mastik F, Garg S et al (2010) First-in-man clinical use of combined near-infrared spectroscopy and intravascular ultrasound: a potential key to predict distal embolization and no-reflow? J Am Coll Cardiol 56:314
26. Saeed B, Banerjee S, Brilakis ES (2010) Slow flow after stenting of a coronary lesion with a large lipid core plaque detected by near-infrared spectroscopy. EuroIntervention 6:545
27. Kilic ID, Caiazzo G, Fabris E, Serdoz R, Abou-Sherif S, Madden S et al (2015) Near-infrared spectroscopy-intravascular ultrasound: scientific basis and clinical applications. Eur Heart J Cardiovasc Imaging 16:1299–1306
28. Morishima I, Sone T, Okumura K, Tsuboi H, Kondo J, Mukawa H et al (2000) Angiographic no-reflow phenomenon as a predictor of adverse long-term outcome in patients treated with percutaneous transluminal coronary angioplasty for first acute myocardial infarction. J Am Coll Cardiol 36:1202–1209
29. Brosh D, Assali AR, Mager A, Porter A, Hasdai D, Teplitsky I et al (2007) Effect of no-reflow during primary percutaneous coronary intervention for acute myocardial infarction on six-month mortality. Am J Cardiol 99:442–445
30. Yajima J (2013) What imaging modality do you want to select for prediction of the no-reflow phenomenon? J Cardiol 62:138–139
31. Katayama T, Kubo N, Takagi Y, Funayama H, Ikeda N, Ishida T et al (2006) Relation of atherothrombosis burden and volume detected by intravascular ultrasound to angiographic no-reflow phenomenon during stent implantation in patients with acute myocardial infarction. Am J Cardiol 97:301–304
32. Sato H, Iida H, Tanaka A, Tanaka H, Shimodouzono S, Uchida E et al (2004) The decrease of plaque volume during percutaneous coronary intervention has a negative impact on coronary flow in acute myocardial infarction: a major role of percutaneous coronary intervention-induced embolization. J Am Coll Cardiol 44:300–304
33. Lee SY, Mintz GS, Kim SY, Hong YJ, Kim SW, Okabe T et al (2009) Attenuated plaque detected by intravascular ultrasound: clinical, angiographic, and morphologic features and post-percutaneous coronary intervention complications in patients with acute coronary syndromes. JACC Cardiovasc Interv 2:65–72
34. Okura H, Taguchi H, Kubo T, Toda I, Yoshida K, Yoshiyama M et al (2007) Atherosclerotic plaque with ultrasonic attenuation affects coronary reflow and infarct size in patients with acute coronary syndrome: an intravascular ultrasound study. Circ J 71:648–653
35. Gamou T, Sakata K, Matsubara T, Yasuda T, Miwa K, Inoue M et al (2015) Impact of thin-cap fibroatheroma on predicting deteriorated coronary flow during interventional procedures in acute as well as stable coronary syndromes: insights from optical coherence tomography analysis. Heart Vessels 30:719–727
36. Hara H, Tsunoda T, Moroi M, Kubota T, Kunimasa T, Shiba M et al (2006) Ultrasound attenuation behind coronary atheroma without calcification: mechanism revealed by autopsy. Acute Card Care 8:110–112
37. Yamada R, Okura H, Kume T, Neishi Y, Kawamoto T, Watanabe N et al (2007) Histological characteristics of plaque with ultrasonic attenuation: a comparison between intravascular ultrasound and histology. J Cardiol 50:223–228
38. Brilakis ES, Abdel-Karim A-RR, Papayannis AC, Michael TT, Rangan BV, Johnson JL et al (2012) Embolic protection device utilization during stenting of native coronary artery lesions with large lipid core plaques as detected by near-infrared spectroscopy. Catheter Cardiovasc Interv 80:1157–1162
39. Young JJ, Kereiakes DJ, Rabinowitz AC, Ammar R, Boucher FL, Rogers C (2005) A novel, low-profile filter-wire (Interceptor) embolic protection device during saphenous vein graft stenting. Am J Cardiol 95:511–514
40. Kotani J, Nanto S, Mintz GS, Kitakaze M, Ohara T, Morozumi T et al (2002) Plaque gruel of atheromatous coronary lesion may contribute to the no-reflow phenomenon in patients with acute coronary syndrome. Circulation 106:1672–1677
41. Uetani T, Amano T, Ando H, Yokoi K, Arai K, Kato M et al (2008) The correlation between lipid volume in the target lesion, measured by integrated backscatter intravascular ultrasound, and post-procedural myocardial infarction in patients with elective stent implantation. Eur Heart J 29:1714–1720
42. Tanaka A, Imanishi T, Kitabata H, Kubo T, Takarada S, Tanimoto T et al (2009) Lipid-rich plaque and myocardial perfusion after successful stenting in patients with non-ST-segment elevation acute coronary syndrome: an optical coherence tomography study. Eur Heart J 30:1348–1355
43. Nakazawa G, Tanabe K, Onuma Y, Yachi S, Aoki J, Yamamoto H et al (2008) Efficacy of culprit plaque assessment by 64-slice multidetector computed tomography to predict transient no-reflow phenomenon during percutaneous coronary intervention. Am Heart J 155:1150–1157
44. Uetani T, Amano T, Kunimura A, Kumagai S, Ando H, Yokoi K et al (2010) The association between plaque characterization by CT angiography and post-procedural myocardial infarction in patients with elective stent implantation. JACC Cardiovasc Imaging 3:19–28
45. Stone GW, Maehara A, Muller JE, Rizik DG, Shunk KA, Ben-Yehuda O et al (2015) Plaque characterization to inform the prediction and prevention of periprocedural myocardial infarction during percutaneous coronary intervention: the CANARY trial (coronary assessment by near-infrared of atherosclerotic rupture-prone yellow). JACC Cardiovasc Interv 8:927–936
46. Yonetsu T, Suh W, Abtahian F, Kato K, Vergallo R, Kim SJ et al (2014) Comparison of near-infrared spectroscopy and optical coherence tomography for detection of lipid. Catheter Cardiovasc Interv 84:710–717